Visible Light Multi-Gb/s Transmission Based on Resonant Cavity LED with Optical Energy Feed

Bernhard Schrenk, *Member, IEEE,* Markus Hofer, *Student Member, IEEE,*
Fabian Laudenbach, Hannes Hübel, and Thomas Zemen, *Senior Member, IEEE*

***Abstract*— Multi-Gb/s visible light communication is demonstrated using a commercial off-the-shelf resonant-cavity light emitting diode, which is originally rated for 150 Mb/s. By applying analog frequency response equalization and multi-carrier modulation schemes, a transmission capacity of up to 4.3 Gb/s is obtained over a single wavelength in a close-proximity scenario. Nyquist-shaped multi-band modulation and orthogonal frequency division multiplexing are applied with high spectral sub-carrier efficiencies of up to 8 bits/symbol. The transmission rate is experimentally investigated as a function of the loss budget and further related to link reach based on free-space measurements under clear weather conditions. Analog signal transmission is also validated using real-time signal (de-)modulation with a high-definition video payload. We further demonstrate that on-off keying in combination with simpler baseband modulation can be facilitated for data rates of up to 750 Mb/s. This proves that commercially available light emitting diodes can serve as versatile low-cost transmitter. Finally, the joint transmission of energy and data has been validated. A power feed with an irradiance of 240 W/m^2 is experimentally shown to enable a remotely supplied optical burst receiver for periodic access to Gb/s data rates.**

***Index Terms*— Optical transmitters, Free-space optical communication, Visible light communication, Light emitting diodes, Modulation, Energy harvesting**

I. Introduction

WIRELESS CONNECTIVITY has become the most important sector of telecommunications. Radio frequency (RF) technology has rapidly evolved during the past decades and has undoubtedly secured its prevalence in this field; however, limitations apply in certain cases such as harsh environments, backhaul links seeking for high transmission capacity or spectrally over-occupied regions. The incomparably low data rates of purely RF-based systems alongside with high latency, low energy efficiency and lack of security of RF-based access are propelling optical wireless links [1]. Moreover optical free-space communications do not suffer from spectral exhaustion, regulation or electro-magnetic interference phenomena as it applies to RF-based communications. The latter result from the typically strong confinement of optical signals in terms of beam divergence and the line-of-sight prerequisite for optical links, which further enhances the security of such communication channels. Although optics has the potential to outperform wireless technology with respect to the aforementioned impediments, it is apparently associated to high cost.

Impressive strides have been made during recent years in order to demonstrate economically viable opto-electronic transceiver components. Latest research work has recently demonstrated 5 Gb/s transmission using a tailored light emitting diode (LED) prototype and multi-carrier formats employing high spectral efficiencies per sub-carrier [2] or multi-level signals and exhaustive electronic equalization [3]. Higher data rates towards 10 Gb/s can be facilitated by means of wavelength division multiplexing as shown with up to four emission wavelengths [4-6], while laser-based visible light communication is anticipated to deliver massive capacities well beyond 10 Gb/s [7-11].

In this work we experimentally demonstrate high data-rate transmission in short reach applications using commercial LED technology. For the first time, 4.3 Gb/s connectivity is achieved with an off-the-shelf resonant-cavity LED rated for a data rate of 150 Mb/s according to its nominal bandwidth resulting from expected process variations during manufacturing. We further show that simple on-off keying at 750 Mb/s and analog signal transmission of multi-carrier signals can be achieved, which is evidenced by real-time transmission of high-definition video payloads. Moreover, the extension to remotely powered optical reception terminals at such high data rates is experimentally demonstrated for the first time.

The manuscript is organized as follows. Chapter II characterizes the LED device as key element in the optical link. Chapter III highlights the methodology used for experimental performance evaluation, for which results are presented in Chapter IV. The joint transmission of energy and data for remote powering of the optical receiver is discussed in Chapter V. Finally, Chapter VI draws the conclusions.

II. Characterization of Resonant-Cavity LED As Directly Modulated Optical Transmitter

Laser technology has matured during the past years and has fertilized a variety of telecom and datacom applications

Manuscript received February22, 2017. This work was supported in part by the European Commission through the FP7 Marie Curie Career Integration Grant WARP-5 under Grant n° 333806.

B. Schrenk, M. Hofer, F. Laudenbach, H. Hübel and T. Zemen are with the Austrian Institute of Technology, Center for Digital Safety&Security, Donau-City Strasse 1, 1220 Vienna, Austria (phone: +43 50550-4131; fax: -4190; e-mail: bernhard.schrenk@ait.ac.at).

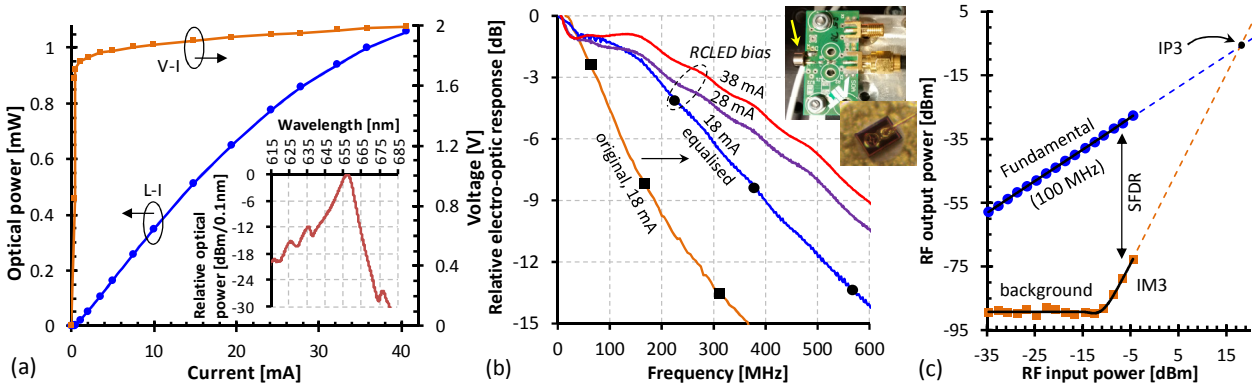

Fig. 1. (a) VLI characteristics of the RCLED and its emission spectrum. (b) Modulation bandwidth before and after analog equalization. (c) Measurement of inter-modulation distortions for the RCLED-based link with PIN receiver.

TABLE I
EVALUATION SCENARIOS

Modulation and Transmitter		Channel	Receiver	Results	
				Chapter	Figure
Nyquist FDM	α	F	A_1	IV.A	4
	α	F	A_2		5(c)
	α	F	A_1 + energy feed	V	8
wide-band OFDM	α	F	A_1	IV.B	6
	α	M	A_1		5(b)
narrow-band OFDM	β	F	B	IV.C	7
Baseband	γ	F	Γ	IV.D	6(c)

The representations for transmitter, channel and receiver refer to the specific implementations shown in Fig. 2.

building on opto-electronic conversion. The coherent light source with its high photon flux, narrow emission spectrum and high coupling efficiencies poses an ideal transmitter for high data rate applications. However, the vulnerability to optical back-reflections and other phenomena of free-space channels, such as scintillations, puts incoherent light sources into the spotlight. LEDs not only provide a low-cost alternative with high lifetime but are also far less susceptible to propagation effects in free-space channels. Originally destined for illumination purposes in the visible-light range, re-use of lighting equipment is thinkable for in-door communication purposes in the low Gb/s range [4, 5]. Visible light can further ease pointing between transmitter and receiver while its incoherence contributes to eye safety. The use of the visible wavelength region also allows for cost-effective silicon detector technology. On the other hand, the applicability of LED technology for fiber-based communication systems is impaired by the low fiber coupling efficiency of incoherent light sources [12]. Besides, the wide emission spectrum of LEDs leads to modal dispersion under fiber-based channels, therefore limiting the transmission capacity to values far below these offered by laser-based sources.

A compromise can be found with the resonant-cavity LED (RCLED) as it was briefly introduced in a recent work [13]. By introducing a resonator structure while keeping the reflectivity small enough not to cause operation as laser, both a narrow spectrum and spatial directionality offering a small radiation angle can be obtained while detrimental propagation effects and multi-path phenomena due to coherence of the output light are avoided. Such an approach for the transmitter is followed in this work. The employed electro-optic converter for light generation and direct modulation is based on the Roithner Lasertechnik RC-LED-650 resonant-cavity LED packaged in a transistor-outline (TO) can. The voltage and light output vs. current (VLI) characteristics of the RCLED are presented in Fig. 1(a). The RCLED features threshold-less operation and shows an optical output power of 0 dBm at a bias current of 36 mA. The emission spectrum, which is shown as inset in Fig. 1(a), is centered at 657 nm and has a full-width half-maximum (FWHM) bandwidth of 6.9 nm. A high electro-optic modulation bandwidth is paramount for the directly modulated emitter when addressing an application such as data transmission. As can be seen in Fig. 1(b), the original (■) response of the RCLED features a -3 dB modulation bandwidth of 75 MHz at a bias current of 18 mA, which prevents the use of this packaged RCLED at high data rates. By applying passive frequency response equalization with a simple T-type RLC RF-circuit, a 2.4-fold improvement in modulation bandwidth is obtained (●). Moreover, there is no strong ripple experienced, which is especially important in case of baseband modulation where no sub-channel adaptation on a frequency-selective basis can be made. The resulting modulation bandwidth of 190 MHz for this particular commercial off-the-shelf device corresponds to typical values found previously for RCLED prototypes [14-16]. The moderate roll-off of -2.8 dB/100 MHz can further suit multi-carrier modulation schemes that slice transmission bandwidth and adapt their bit loading accordingly.

The analog optical transmission of multi-level or multi-carrier data signals further necessitates linear opto-electronic converters. As an important metric of linearity, intermodulation distortion measurements have been conducted for the RCLED-based link with PIN receiver. Two closely spaced RF tones have been injected into the transmitter as stimulus, which produces additional frequency components in case of non-linearity. This spectral content becomes

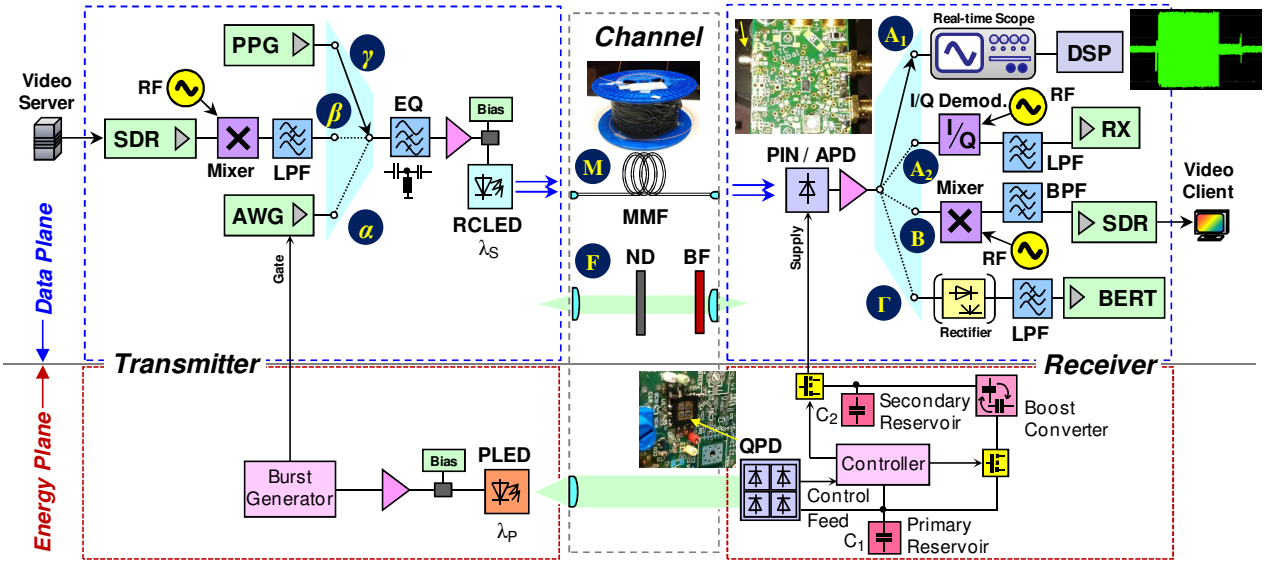

Fig. 2. Experimental setup to evaluate the performance of the RCLED-based transmitter under various scenarios, including remote energy feeding.

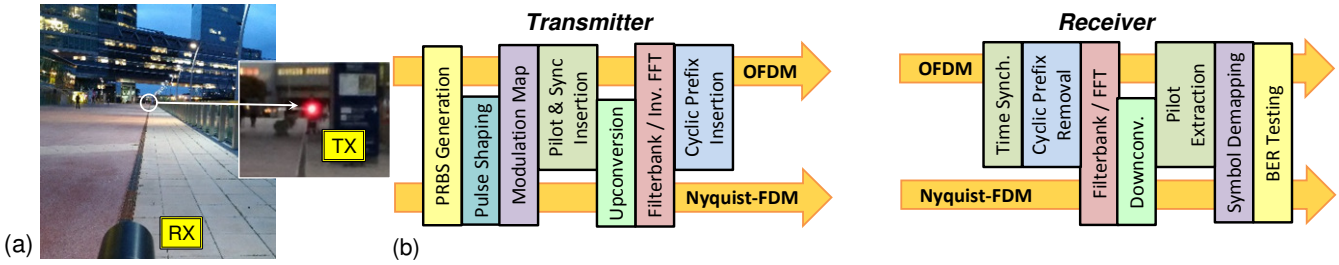

Fig. 3. (a) Free-space setup to correlate loss budget and reach. (b) DSP stacks employed at transmitter and receiver.

challenging in case of third-order intermodulation (IM3) distortion adjacent to the two-tone input since these distortions can deteriorate the signal of interest. The power ratio between fundamental tones and IM3 products describes the spurious-free dynamic range (SFDR). A high SFDR of 45 dB at a RF input power of -5 dBm was obtained (Fig. 1(c)). However, the SFDR depends on the RF input power as the IM3 products grow faster than the fundamental stimulus when increasing the RF input power level. For this reason the related third-order interception point (IP3) is considered as additional figure of merit. This point corresponds to an arbitrarily high RF input power level for which the SFDR becomes 0 dB in case that no saturation effects would occur, meaning that the IM3 products would intercept the fundamental stimulus in terms of RF power level. The input IP3 point for the optical link is 17.8 dBm, which renders the RCLED as a suitable analog electro-optic modulator.

III. Experimental Evaluation Methodology

In order to evaluate the feasibility of the RCLED-based link under various scenarios, the experimental performance was evaluated under different modulation and detection techniques featuring also different transmission channels. Table I lists the cases considered for evaluation, which are explained in more detail in the following sub-sections.

A. Experimental Setup

The experimental setup is depicted in Fig. 2. Three data transmission schemes have been investigated, for which the RCLED was driven by either an arbitrary waveform generator (AWG) for wideband multi-carrier modulation (α in Fig. 2), a software-defined radio (SDR, β) whose narrowband multi-carrier signal was down-converted to an intermediate frequency (IF), or a pulse-pattern generator (PPG) for baseband modulation (γ). The analog RF equalizer (EQ) circuit used for extending the modulation bandwidth of the RCLED-based opto-electronic converter was placed at the transmitter, followed by an electrical amplifier that drives the RCLED while also compensating the equalizer circuit losses. The RCLED was biased at 18 mA. Note that the equalizer circuit that is a prerequisite for baseband modulation was kept even for multi-carrier formats in order to retain the same conditions for the transmitter.

The optical channel between transmitter and receiver was implemented by either a free-space path (F) or a fiber-based link (M). For the latter, a gradient-index multi-mode fiber (MMF) with a 62.5 µm core diameter and a length of up to 1 km was used. In case of the free-space path, the optical loss between RCLED and receiver was varied by means of neutral density (ND) filters inserted in the 10 cm light path between transmitter and receiver. In this way, the dependence of the link data rate on the optical path loss budget was investigated. An evaluation over transmission loss rather than range was preferred since the latter typically depends on the exact optical system used for beam collimation and weather conditions in case of out-door links. Nonetheless, free-space measurements

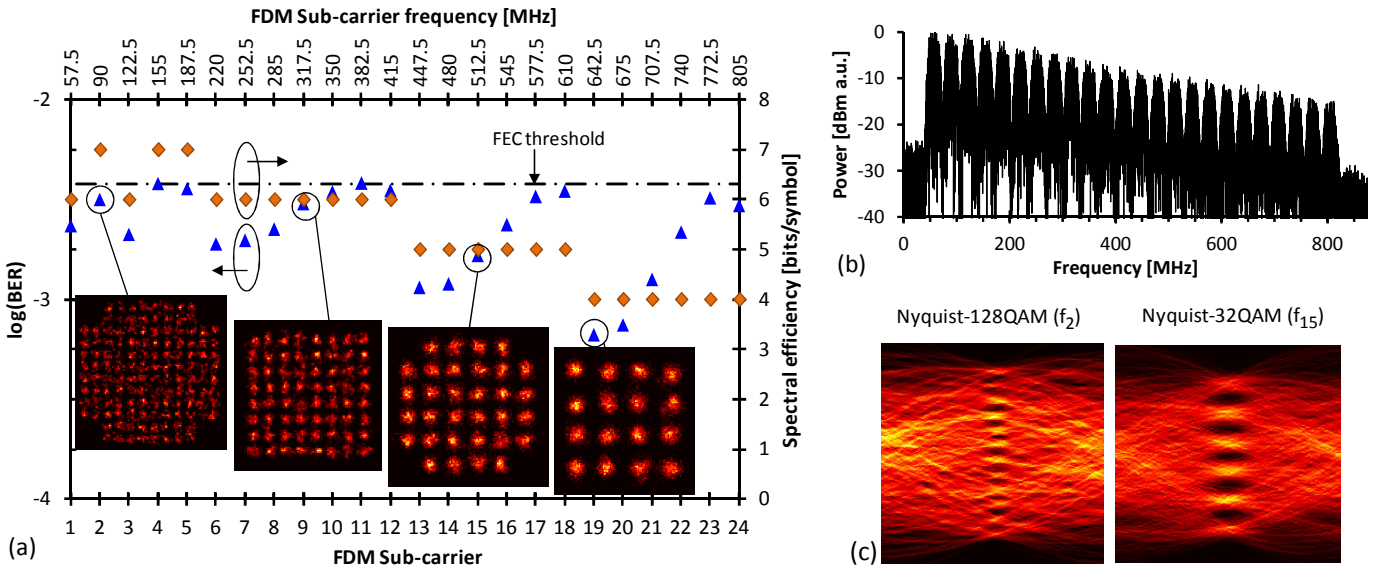

Fig. 4. (a) BER performance and spectral efficiency for Nyquist-FDM. (b) Received spectrum. (c) Eye diagrams for one I/Q tributary of sub-carriers 2 and 15.

have been conducted during clear weather using mobile measurement equipment in order to relate loss and reach in a realistic scenario (Fig. 3(a)). For this purpose, a long-pass filter (BF) with a filter edge at 655 nm suppressing background light has been additionally inserted in front of the receiver. It shall be noted that no fixed installation was available for the free-space link, which prevented the placement of large lab instruments such as arbitrary waveform generators or real-time oscilloscopes. Moreover, extra losses need to be taken into consideration in case of severe weather conditions [17].

At the receiver site, the optical signal is coupled to either a PIN photodiode or an avalanche photodiode (APD). A bias voltage corresponding to a multiplication factor of 10 was set for the APD. The opto-electronic reception bandwidth for photodiode and transimpedance amplifier was ~1 GHz and 650 MHz for PIN- and APD-based optical receiver, respectively. The detected signal is then acquired by an electrical sink depending on the applied modulation scheme. In case of wideband multi-carrier modulation, a real-time storage oscilloscope (A_1 in Fig. 2) for subsequent off-line digital signal processing (DSP) or an I/Q demodulator with local oscillator (A_2) for DSP-less reception of the I/Q baseband data has been used. In case of narrowband multi-carrier modulation for real-time error estimation, a SDR receiver with preceding IF up-converter was applied (B). A bit error ratio tester (BERT) was used to conduct direct BER measurement in case of baseband modulation (Γ).

Several transmitter/receiver combinations used for evaluation are summarized in Table I. An extension of the data plane shown in Fig. 2 by an energy feeding mechanism for remote powering of the optical receiver is separately discussed in Section V.

B. Modulation Formats

Three multi-carrier formats have been selected for performance evaluation. The first is a frequency division multiplexed (FDM) format employing Nyquist-shaped quadrature amplitude modulation (QAM). Such a modulation scheme can be beneficial when spectrum is seen as a scarce resource while multi-band access schemes are to be implemented in combination with point-to-multipoint connectivity with technologically lean user terminal equipment based on simple, DSP-less reception without the need for broadband electronics. The Nyquist-FDM consists of up to 24 sub-carriers, which are individually loaded at a symbol rate of 25 MHz having optimal spectral efficiency setting according to the received signal-to-noise ratio, which has been acquired before data transmission by means of channel sounding. A sub-channel spacing of 32.5 MHz was chosen as the best trade-off between sub-channel separation and spectral occupancy. This separation enables a low-complexity (passband) receiver to select a particular sub-channel without being affected by severe crosstalk from neighbors.

Orthogonal frequency division multiplexing (OFDM) has been selected as second modulation scheme for superior spectral efficiency and occupancy, leading to an optimal use of precious modulation bandwidth. In total, 256 sub-carriers have been spanned over a modulation bandwidth of up to 1 GHz for low optical loss budgets. Hermitian symmetry was used to yield a real-valued signal for subsequent multi-carrier modulation in the baseband at the aforementioned DC bias. The QAM format for the 248 data sub-carriers has been again adapted to the channel response and optical path loss, as for the Nyquist-FDM. The DSP stacks for Nyquist-FDM and OFDM modulation at transmitter and receiver are included in Fig. 3(b).

The third format used in the experiment is a narrowband OFDM as applied in radio or powerline communication systems. The OFDM signal used in this work had 64 sub-carriers over a modulation bandwidth of 20 MHz. The OFDM

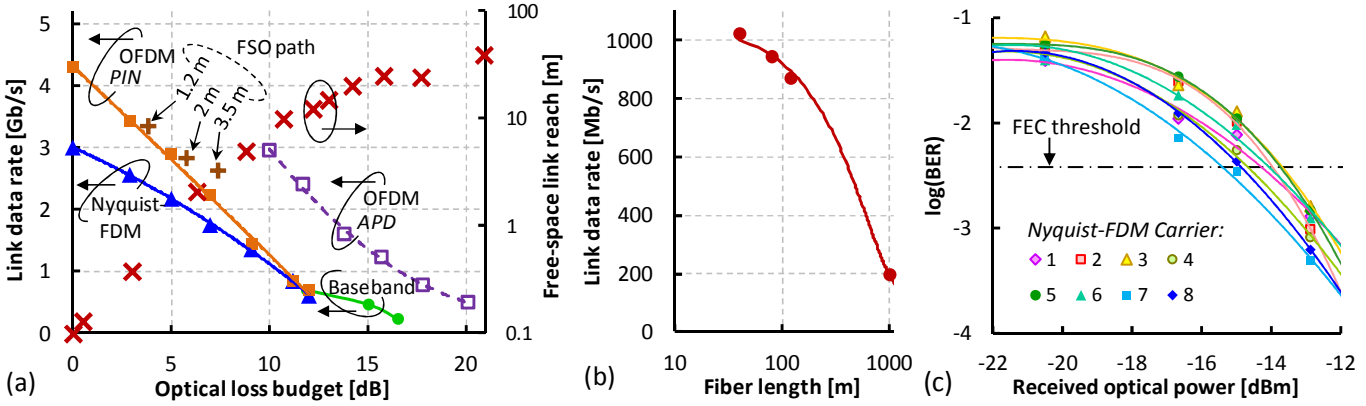

Fig. 5. (a) Nyquist-FDM, OFDM and baseband rates for various optical loss budgets. (b) OFDM link rate of multi-mode fiber. (c)BER for analog down-conversion of Nyquist-FDM channels.

signal at a carrier frequency of 4.6 GHz has been converted to an IF of 480 MHz for use with the RCLED-based link. Real-time transmission has been implemented on the NI USRP-2953R SDR and is used in combination with high-definition video streaming at an image resolution of 1280×720p.

Finally, the RCLED-based transmitter has been also evaluated for baseband modulation with a PPG/BERT set, which does not require DSP functionality at transmitter or receiver. This case is especially interesting when energy-conscious links with low implementation complexity are sought for.

IV. Experimental Results

A. *Multi-carrier transmission based on Nyquist-FDM*

Multi-carrier transmission (configuration α-F-A_1 in Fig. 2) with closely-spaced FDM channels amenable for analog demultiplexing serves as the first scenario for performance evaluation. Firstly, the back-to-back transmission performance with PIN-based receiver was evaluated. This case without additional ND filters corresponds to an optical power of -2.9 dBm impinging onto the receiver, as it was acquired with a free-space power meter. Results are shown in Fig. 4(a) for several sub-channels. 128-QAM with a corresponding spectral efficiency (♦) of 7 bits/symbol can be supported for lower sub-channels at a BER (▲) below the forward error correction (FEC) level, for which a threshold of 3.8×10^{-3} was chosen. This proves that the RCLED as low-cost transmitter suits rather wide sub-channel bandwidths without being affected due to distortions arising from excessive ripple at the electro-optic response. With the given bit loading, an aggregated pre-FEC transmission capacity of 3.23 Gb/s is achieved over all 24 sub-channels spanning up to 805 MHz (Fig. 4(b)). The spectral efficiency averaged over all sub-channels is 5.38 bits/symbols. The net data rate is 3 Gb/s after accommodating for the typical 7% overhead of hard-decision FEC.

The eye diagrams for one I/Q tributary at sub-channels 2 and 15, carrying 128- and 32-QAM respectively, are depicted in Fig. 4(c) and show the characteristic Nyquist pulse shaping. The eye opening can be clearly observed even in case of 128-QAM, evidencing the viability of this sensitive format for transmission over the RCLED-based link.

The Nyquist-FDM performance for increased optical loss budget emulated through insertion of ND filters is presented in Fig. 5(a). The optical budget is referenced to the back-to-back case, meaning a coupled optical power of -2.9 dBm at the receiver. The obtained Nyquist-FDM data rate (▲) decreases with 0.2 Gb/s/dB when increasing the loss budget, leading to 1 Gb/s transmission at a compatible loss budget of 10.8 dB, corresponding to a received optical power of -13.7 dBm.

DSP-aided receiver implementations can be avoided by introducing passband receivers that utilize analog down-conversion of a specific sub-channel (configuration α-F-A_2). Such a reception scheme has been evaluated in combination with the APD-based receiver and a Nyquist-FDM signal comprising of 8 sub-channels from 252.5 to 480 MHz. Each of sub-carriers was modulated at a fixed 16-QAM format in order to yielding 100 Mb/s throughput per sub-channel. Since the channel response of the optical link differs for the particular sub-carriers, power loading has been performed to provide a similar reception performance for all sub-channels. A BER below the FEC level has been obtained after multi-level symbol slicing for all of the sub-channels for a loss budget of 11.5 dB. Figure 5(c) indicates a residual spread of 1.4 dB in reception sensitivity at the FEC level, which is explained by the frequency-dependent detection performance of the analog I/Q demodulator used after the optical receiver. The use of an analog reception methodology guarantees simplicity and low cost and can co-exist with DSP-based broadband reception in a potential multi-user scenario.

B. *Wide-band OFDM transmission*

When a single data signal of a single user is to be transmitted, the channel can be exclusively exploited by the corresponding modulation format. Wide-band OFDM transmission (configuration α-F-A_1) using the entire modulation bandwidth of the optical link has been evaluated in this context. The performance for the back-to-back case with PIN-based receiver is shown in Fig. 6(a). The spectral efficiency can be further increased with respect to Nyquist-FDM due to the finer granularity with which the transmission spectrum is resolved. 256-QAM performance below the FEC threshold is achieved for part of the lower sub-carriers. The aggregated data rate

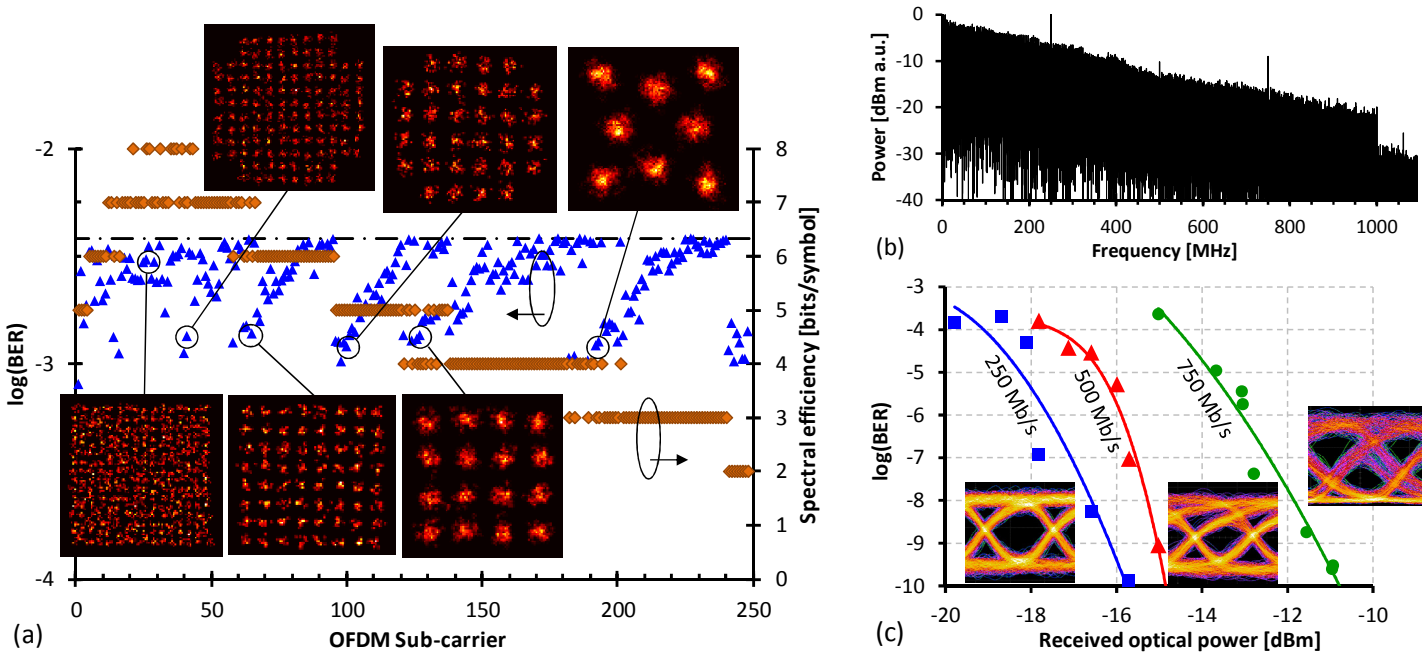

Fig. 6. (a) BER performance and spectral efficiency for OFDM modulation. (b) Received spectrum. (c) BER performance for baseband on-offkeying.

obtained is 4.62 Gb/s after cyclic prefix removal. The average spectral efficiency is 4.87 bits/symbol. Even this is lower compared to Nyquist-FDM, the wider OFDM modulation bandwidth of 1 GHz (Fig. 6(b)) and the higher spectral occupancy result in a higher throughput. On the other hand, unlike the case of slicing Nyquist-FDM with a bandpass receiver, detection has to be conducted with a broadband receiver in case of OFDM. Taking into account the overhead for error correction, the post-FEC data rate amounts to 4.3 Gb/s. In terms of sensitivity to optical path loss the wideband OFDM data rate decreases with 0.31 Gb/s/dB and reaches 1 Gb/s at an optical budget of 11 dB (Fig. 5(a), ■).

The link data rate has been further evaluated for the three indoor link reaches of 1.2, 2 and 3.5 m rather than solely using ND filters for loss budget emulation. The obtained rates are introduced in Fig. 5(a), +, and are plotted for the respective loss budget that is related to the corresponding reach as estimated from the free-space measurements (×). The obtained indoor link rates agree with these obtained when emulating an increased loss budget in the foregoing short-reach link (■).

When using the APD-based receiver, the compatible loss budget extends by ~5.3 dB and reaches a value of 16.6 dB for a data rate of 1 Gb/s (Fig. 5(a), □). This extension in link data rate for a given loss budget is explained by the multiplication factor contributed by the APD, which however does not translate into a similar capacity-wise improvement in loss budget due to the reduced reception bandwidth of the APD. Reach-wise a distance of 24 m can be anticipated for this loss budget from the free-space measurements (Fig. 5(a), ×), for which a directed optical beam at clear weather conditions applies rather than an illumination scenario. It shall be noted that beam formation and steering of incoherent LED light for dynamic focusing and deflection towards (a potentially mobile) receiving target has been experimentally shown previously [18-20].

As an alternative to free-space based communication a fiber channel can act as relay towards an optical hotspot (configuration α-M-A_1). The coupling of incoherent light to the optical fiber determines the link loss and with it the maximum achievable link data rate of 1 Gb/s for a short multi-mode fiber of 40 m (Fig. 5(b)). When increasing the length of the fiber, its kilometric attenuation of 13.8 dB/km that results from the large scattering losses in the visible light region reduces the data rate to 197 Mb/s for the longest fiber span of 1 km.

C. *Real-time narrow-band OFDM transmission*

Besides wideband OFDM, a single-channel narrowband OFDM transmission (configuration β-F-B) at the IF of 480 MHz has been evaluated in terms of block error ratio (BLER) measurements with a payload size of 9024 bits/packet. Different sub-carrier modulation formats and convolutional code rates *R* have been investigated (Fig. 7(a)). When using the PIN-based receiver, 54 Mb/s 64-QAM OFDM with R=3/4 is supported up to a loss budget of 5 dB, for which a BLER of 10^{-2} is reached. Higher loss budgets of up to 10 dB can be supported through 16-QAM subcarrier modulation. With the APD-based receiver, the sensitivity improves by 9.7 to 10.2 dB in good agreement to the multiplication factor of the APD. A loss budget of 16 dB is found for 64-QAM OFDM and a BLER of 10^{-2} (▲). This corresponds to a free-space reach of ~22 m (Fig. 5(a), ×).

Real-time streaming of HDTV video content (Fig. 7(b)) has been performed without the notice of visual artifacts, which is also evidenced by the clear constellation diagrams shown in Fig. 7(a).

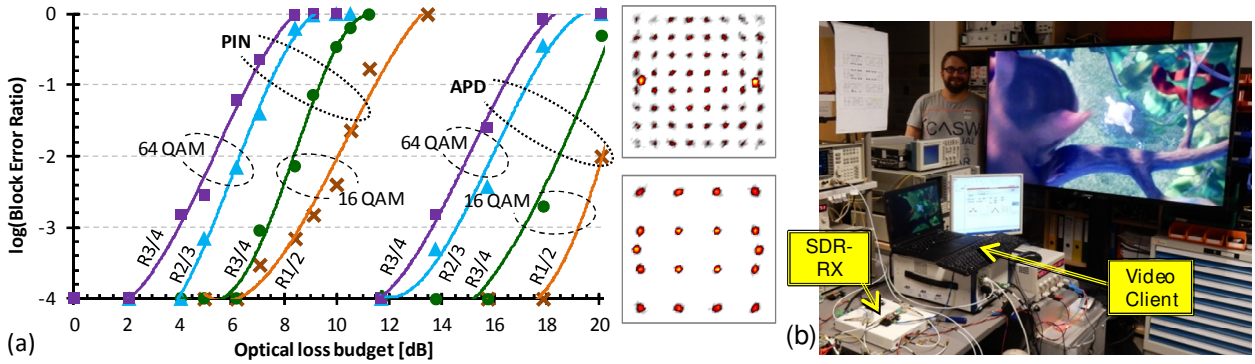

Fig. 7. (a) BLER over optical loss budget for real-time narrow-band OFDM reception. Signal constellations are shown for the PIN-based receiver. (b) High-definition video streaming over RCLED-based link.

D. *Baseband modulation*

In the fourth transmission scheme, on-off keying (configuration γ-F-Γ) has been performed at three different data rates of 250, 500 and 750 Mb/s. In order to facilitate the highest data rate of 750 Mb/s with the given electro-optic bandwidth of 190 MHz for the RCLED, a rectifier has been inserted after the PIN-based receiver serving as duobinary-to-binary signal converter. In this way, the duobinary signal, which is generated by the RCLED having a response close to a 4^{th}-order Bessel filter at a quarter of the bit rate, is transformed into the original on-off keyed signal [21].

Figure 6(c) shows the BER performance for all transmission rates. A low BER of 10^{-10} can be reached for several rates, which is evidenced by the clear eye opening. With reference to commonly used FEC thresholds at 2×10^{-4}, the compatible loss budgets are 16.5 (■), 14.9 (▲) and 11.9 (●) dB for data rates of 250, 500 and 750 Mb/s, respectively. With this, the data rate of baseband modulation is found to decrease by 0.11 Gb/s/dB when increasing the optical loss budget (Fig. 5(a), ●). The capability of the RCLED to perform error-free opto-electronic conversion in combination with baseband modulation enables the optical transmitter to serve in a more energy-efficient mode in case of lower throughput.

It shall be stressed that the performance of the 250 Mb/s transmission (■) is compromised by the unavailability of a suitable low-pass filter (LPF) below 500 MHz to cut electrical noise before the BERT.

V. Remote Powering of the Optical Receiver

In certain cases where low-power applications are considered, energy self-sufficient sub-systems are of special interest. These can be, for example, sensor applications or communication equipment with sporadic access to data, instructions or synchronization signals. Rather than deploying a costly power supply for these low-power devices, the required energy for exchange of information can then be either harvested from the surrounding or fed from a remote source.

For the particular case of optical wireless communication, the challenge resides in supplying the user terminal through the communication channel. Such an approach has been recently demonstrated by employing solar-cell like detectors capable to receive energy and data streams with data rates up to 12 Mb/s [22,23]. In this work, we employ an optical detector as simultaneous energy harvester and wake-up receiver to facilitate higher burst data rates in the Gb/s regime as demonstrated in Section IV.

The concept was validated with an auxiliary energy feeding and signaling channel in parallel to the short-reach data channel investigated earlier. For this reason, the data plane in Fig. 2 was extended by an energy plane comprising an energy source at the transmitter and an energy-harvesting sub-system at the receiver. In similarity to a recent work on remotely powered network nodes for fiber-based access networks [24], the energy feed is provided through a high-power LED (PLED) emitting at λ_P = 850 nm. The collimated pump beam illuminates a quad photodetector (QPD) at the receiver with an irradiance of 240 W/m^2. Data and energy channel were spatially separated so that the pump does not fall in the field-of-view of the data receiver. The QPD opto-electronically harvests the energy for the operation of the high-bandwidth PIN-based data receiver requiring a supply of 90 mA at 2.1V. The QPD has a responsivity of 0.45 A/W at λ_P and a fill factor of 39%. It acts as a photovoltaic energy converter that charges a primary supercapacitor (C_1) with a capacity of 33 mF. A boost converter is then used to generate a secondary supply rail at a higher voltage, in compliance with the data receiver. Periodic power cycling for recharging the secondary supply rail after data reception and self-discharge of the secondary 10 mF supercapacitor (C_2) is facilitated through an ultra-low voltage CMOS controller with an idle current of ~2 µA. This controller does also handle signaling between transmitter and receiver, which is integrated on the pump feed with a low modulation extinction ratio of 1 dB (Fig. 8(a)). In case of detecting a trigger signal (A) that indicates the arrival of a data burst at λ_S with specific length (e.g., 4 ms in Fig. 8(a)), the controller activates its data receiver (B) by asserting a respective gate signal. The data burst is then received. The depletion of the stored energy in the secondary supply rail alongside with the activation of the high-bandwidth data receiver results in a droop for the received data burst. The data receiver is then deactivated (C) and the secondary supply rail is re-charged accordingly.

A typical energy cycling and conversion operation following a cold start is depicted in Fig. 8(b). The primary energy reservoir is first charged at τ_0 by the QPD (X) leading

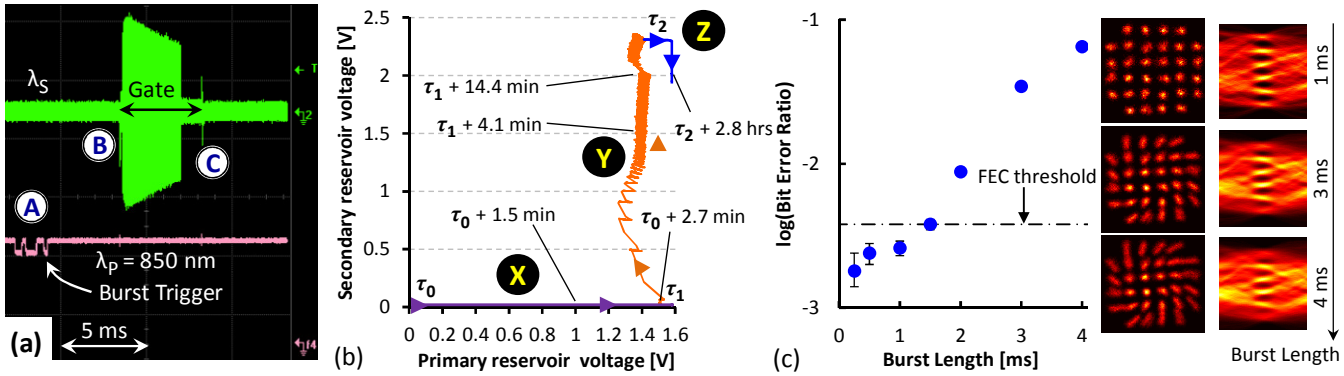

Fig. 8. (a) Burst-mode reception under remote powering of data receiver. (b) Energy scavenging procedure and established power supply rails for the receiving unit. (c) BER and received signal constellations for burst data as function of the burst length utilizing a remotely-fed receiver.

to a primary supply rail at 1.5V after 2.7 min. This is enough to periodically cycle a capacitive boost converter (Y) to charge the secondary energy reservoir at τ_1 to establish its secondary supply rail with up to 2.3V. This one-time procedure takes 16 min. Self-discharge of the secondary reservoir (Z) after disconnection from the energy feed at τ_2 during an idle cycle of the overall receiving unit amounts to 5% after 42 min and periodically requires a short re-charge operation.

The impact of the remote energy feed on the reception performance has been investigated for data bursts with variable length. A 20-channel Nyquist-FDM format as introduced in Section IV.A has been investigated at a loss budget of 6 dB, for which a reach of 2 m can be anticipated considering a directed optical beam rather than an illumination scenario (Fig. 5(a), ×). The BER shown in Fig. 8(c) relates to 32-QAM modulation at the central sub-channel, for which a BER of 2×10^{-3} is obtained for a locally supplied data receiver. The BER degradation with increased burst length results from the decreasing signal-to-noise ratio along the burst as the supply rail depletes. This effect is visible in the collapsing signal constellations and eye diagrams shown in Fig. 8(c). However, up to a burst length of 1.4 ms a BER below the FEC threshold can be obtained. In view of typically used data packet lengths, as for example applied in access-oriented Gigabit Passive Optical Network (GPON) systems, the feasibility of burst-wise high data-rate transmission is validated. Note that simpler modulation formats towards broadband on-off keying are less vulnerable and can tolerate longer burst lengths in trade-off with a lower data throughput.

In case that data and energy feeding channel are not spatially separated, as it would be the case in longer-range links, appropriate measures need to be considered to mitigate pump crosstalk noise during the reception of data. These can include spectral filtering at the data receiver or temporal blanking of the pump during burst data reception. As suggested by the slow self-discharge (Z) shown in Fig. 8(b), a short interruption in the pump feed can be tolerated in virtue of the receiver's energy storage capability.

It shall be also stressed that the current demonstration assumes an energy autarkic data sink. Given the acceptable performance of QAM modulation, simpler on-off keying can be a viable low-power solution without the need for additional post-processing. However, since the influence of the energy feeding scheme on the transmission performance is more pronounced in case of higher-order modulation formats, the present investigation focused on QAM formats.

VI. Conclusion

A commercial off-the-shelf TO-can RCLED rated for 150 Mb/s has been experimentally demonstrated at multi-Gb/s data rates. Nyquist-FDM and OFDM modulation schemes with adaptive bit loading lead to back-to-back data rates of up to 4.3 Gb/s over a single wavelength. This high data rate, which to our best knowledge is the highest ever shown with commercial LED devices, is facilitated through high-order sub-carrier formats up to 256-QAM. On top of this, frequency response equalization in the analog RF domain allows for baseband modulation using simple on-off keying at data rates of up to 750 Mb/s, for which an optical loss budget of ~12 dB has been found compatible in combination with a simple, PIN-based receiver. Analog real-time transmission of narrow-band 64-QAM OFDM signals with high-definition video payload has been demonstrated over a loss budget of 16 dB, corresponding to a link reach of more than 20 m. These transmission experiments in close-proximity scenarios prove the maturity of commercially available LED technology as optical transmitter for applications in short-reach visible light communication. Finally, the concept of joint energy and data transmission has been validated through the experimental extension of the purely communication-oriented optical link by an energy feed. Gb/s burst-mode rates have been proven feasible in combination with a remotely powered optical receiver and burst lengths of up to 1.4 ms. This opens vistas for energy-autarkic terminals requiring just periodic or sporadic access to information.

Acknowledgment

The authors are gratefully acknowledging Roithner Lasertechnik for supplying the LED device.

References

[1] S. Wu, H. Wang, and C.H. Youn, "Visible Light Communications for 5G Wireless Networking Systems: From Fixed to Mobile Communications," *IEEE Network*, vol. 26, no. 6, pp. 41-45, Nov. 2014.

[2] R. Ferreira *et al.*, "High Bandwidth GaN-Based Micro-LEDs for Multi-Gb/s Visible Light Communications," *IEEE Phot. Technol. Lett.*, vol. 28, no. 19, pp. 2023-2026, Oct. 2016.
[3] J. Vinogradov et al., "GaN Light-Emitting Diodes for up to 5.5-Gb/s Short-Reach Data Transmission Over SI-POF," *IEEE Phot. Technol. Lett.*, vol. 26, no. 24, pp. 2473-2475, Dec. 2014.
[4] G. Cossu, A. Khalid, P. Choudhury, R. Corsini, and E. Ciaramella, "3.4 Gbit/s visible optical wireless transmission based on RGB LED," *OSA Opt. Expr.*, vol. 20, no. 26, pp. B501-B506, 2012.
[5] Y. Wang, L. Tao, X. Huang, J. Shi, and N. Chi, "8-Gb/s RGBY LED-Based WDM VLC System Employing High-Order CAP Modulation and Hybrid Post Equalizer," *IEEE Phot. J.*, vol., no. 6, p. 7904507, Dec. 2015.
[6] H. Chun *et al.*, "LED Based Wavelength Division Multiplexed, 10 Gb/s Visible Light Communications," *J. Lightwave Technol.*, vol. 32, no. 13, pp. 3047-3052, Jul. 2016.
[7] D. Tsonev, S. Videv, and H. Haas, "Towards a 100 Gb/s visible light wireless access network," *OSA Opt. Expr.*, vol. 23, no. 2, pp. 1627-1637, Jan. 2015.
[8] C. Chang *et al.*, "A 100-Gb/s Multiple-Input Multiple-Output Visible Laser Light Communication System," *IEEE/OSA J. Lightwave Technol.*, vol. 32, no. 24, pp. 4121-4127, 2014.
[9] Y. Chi, D. Hsieh, C. Tsai, H. Chen, H. Kuo, and G. Lin, "450-nm GaN laser diode enables high-speed visible light communication with 9-Gbps QAM-OFDM," *OSA Opt. Expr.*, vol. 23, no. 10, pp. 13051-13059, 2015.
[10] A.T. Hussein, M.T. Alresheedi, J.M.H. Elmirghani, "20 Gbps Mobile Indoor Visible Light Communication System Employing Beam Steering and Computer Generated Holograms," *IEEE/OSA J. Lightwave Technol.*, vol. 33, no. 24, pp. 5242-5260, 2015.
[11] A.T. Hussein, M.T. Alresheedi and J.M.H. Elmirghani, "25 Gbps mobile visible light communication system employing fast adaptation techniques," in *Proc. ICTON'16*, Trento, Italy, Jul. 2016, paper Tu.P.17.
[12] C. Yeh, *Handbook of Fiber Optics: Theory and Applications*, Academic Press, 1990, pp. 13-37.
[13] B. Schrenk, M. Hofer, F. Laudenbach, H. Hübel, T. Zemen, "Low-Cost Visible Light Communication System based on Off-the-Shelf LED for up to 4.3 Gb/s/λ Transmission," in *Proc. OFC'17*, Los Angeles, USA, Mar. 2017, paper W3F.5.
[14] M. Guina *et al.*, "Light-Emitting Diode Emitting at 650 nm with 200-MHz Small-Signal Modulation Bandwidth," *IEEE Phot. Technol. Lett.*, vol. 12, no. 7, pp. 786-788, Jul. 2000.
[15] S.W. Chiou, Y.C. Lee, C.S. Chang, T.P. Chen, "High speed red RCLEDs for plastic optical fiber,"*Proc. of SPIE*, vol. 5739, pp. 129-133, Mar. 2005.
[16] C.L. Tsai, Z.F. Xu, "Line-of-Sight Visible Light Communications With InGaN-Based Resonant Cavity LEDs," *IEEE Phot. Technol. Lett.*, vol. 25, no. 18, pp. 1793-1796, Sept. 2013.
[17] S. Bloom, E. Korevaar, J. Schuster, H. Willebrand, "Understanding the performance of free-space optics [Invited]," *J. Opt. Netw.*, vol. 2, no. 6, pp. 178-200, Jun. 2003.
[18] S.M. Kim, S.M. Kim, "Wireless visible light communication technology using optical beamforming," *SPIE Opt. Eng.*, vol. 52, no. 10, 106101, Oct. 2013.
[19] X. Shang, A.M. Trinidad, P. Joshi, J. De Smet, D. Cuypers, H. De Smet, "Tunable Optical Beam Deflection Via Liquid Crystal Gradient Refractive Index Generated By Highly Resistive Polymer Film," *IEEE Phot. J.*, vol. 8, no.3, p. 6500411, Jun. 2016.
[20] T.A. Tran, D. O'Brien, "LED holographic beam-steering for visible-light communications," in *Proc. Globecom'13*, Atlanta, USA, Dec. 2013, pp. 1099-1102.
[21] M. Omella, V. Polo, J.A. Lazaro, B. Schrenk, and J. Prat, "10 Gb/s RSOA Transmission by Direct Duobinary Modulation", in *Proc. ECOC'08*, Brussels, Belgium, Sept. 2008, vol. 2, pp. 121-122.
[22] Z. Wang, D. Tsonev, S. Videv, H. Haas, "On the Design of a Solar-Panel Receiver for Optical Wireless Communications With Simultaneous Energy Harvesting," *IEEE J. Sel. Areas Commun.*, vol. 33, no. 8, pp. 1612-1623, Aug. 2015.
[23] Y. Liu, H.Y. Chen, K. Liang, C.W. Hsu, C.W. Chow, C.H. Yeh "Visible Light Communication Using Receivers of Camera Image Sensor and Solar Cell," *IEEE Phot. J.*, vol. 8, no. 1, p. 7800107, Feb. 2016.
[24] B. Schrenk *et al.*, "Passive ROADM flexibility in optical access with spectral and spatial reconfigurability," *IEEE J. Sel. Areas Commun.*, vol. 33, no. 12, pp. 2837-2846, Dec. 2015.

Bernhard Schrenk (S'10-M'11) was born 1982 in Austria and received the M.Sc. ('07) degree in microelectronics from the Technical University of Vienna. He was at the Institute of Experimental Physics of Prof. A. Zeilinger, where he was involved in the realization of a first commercial prototype for a quantum cryptography system, within the European SECOQC project. From 2007 to early 2011 he obtained his Ph.D degree at UPC BarcelonaTech, Spain. His Ph.D thesis on multi-functional optical network units for next-generation Fiber-to-the-Home access networks was carried out within the FP7 SARDANA and EURO-FOS projects. In 2011 he joined the Photonic Communications Research Laboratory at NTUA, Athens, as post-doctoral researcher and established his research activities on coherent FTTH under the umbrella of the FP7 GALACTICO project. In 2013 he established his own research force on photonic communications at AIT Austrian Institute of Technology, Vienna, where he is working towards next-generation metro-access-5G networks, photonics integration technologies and quantum optics.
Dr. Schrenk has authored and co-authored ~100 publications in top-of-the-line (IEEE, OSA) journals and presentations in the most prestigious and highly competitive optical fiber technology conferences. He was engaged in several European projects such as SARDANA, BONE, BOOM, APACHE, GALACTICO and EURO-FOS. In 2013 he received the European Marie-Curie Integration Grant WARP-5. He was further awarded with the Photonics21 Student Innovation Award and the Euro-Fos Student Research Award for his PhD thesis, honoring not only his R&D work but also its relevance for the photonics industry.

Markus Hofer (S'14) received the M.Sc. degree (with distinction) in telecommunications from the Vienna University of Technology, Vienna, Austria, in 2013. Since 2013, he has been working toward the Ph.D. degree in telecommunications. From 2013 to 2015 he was with the FTW Telecommunications Research Center Vienna working as a Researcher in "Signal and Information Processing" department. Since 2015, he has been with the AIT Austrian Institute of Technology, Vienna, as a Junior Scientist in the research group for ultra-reliable wireless machine-to-machine communications. His research interests include low-latency wireless communications, vehicular channel measurements, modeling and emulation, time-variant channel estimation, cooperative communication systems, and interference management.

Fabian Laudenbach, born 1985 in Vienna, Austria, studied theoretical physics at the University of Vienna. He graduated as M.Sc. in the field of quantum optics and quantum information in 2015.
Mr. Laudenbach has been with the Austrian Institute of Technology since 2014 where he is currently working towards his PhD degree. His field of interest comprises theoretical and experimental quantum cryptography, optical metro-access networks, quantum optics as well as theoretical and computer-based research on the interface of non-linear optics and quantum information.

Hannes Hübel obtained his Ph.D. in physics in 2004 at Queen Mary, University of London (UK). After completing his PhD he joined the group of Prof. Zeilinger at the University of Vienna (Austria) as a postdoctoral researcher to work on entanglement based quantum key distribution. From 2007 onwards, he was group leader of the QKD group and supervised the realization and demonstration of a fully functioning autonomous entanglement-based QKD device as part of the European SECOQC project. In 2009 he moved to the Institute for Quantum Computing at the University of Waterloo (Canada) as a postdoctoral fellow and worked with Prof. Jennewein on generation of photon triplets from parametric downconversion as well as fiber and satellite based QKD. In 2011 he became an assistant professor at the physics department of the Stockholm University

(Sweden), where he worked on long-distance fiber-based quantum information technologies at telecommunication wavelengths. Since 2015 he is at the Austrian Institute of Technology in Vienna (Austria) heading the Optical Quantum Technology unit.
Dr. Hübel has authored and co-authored more than 80 publications and contributions in high impact (Nature, PRL) journals and international conferences on Quantum Information. His current research activities include quantum communication with discrete and continuous variables as well as photon-pair generation in photonic integrated circuits.

Thomas Zemen (S'03-M'05-SM'10) received the Dipl.-Ing. degree (with distinction) in electrical engineering in 1998, the doctoral degree (with distinction) in 2004 and the Venia Docendi (Habilitation) for "Mobile Communications" in 2013, all from Vienna University of Technology.
From 1998 to 2003 he worked as Hardware Engineer and Project Manager for the Radio Communication Devices Department, Siemens Austria. From 2003 to 2015 Thomas Zemen was with FTW Telecommunications Research Center Vienna and Head of the "Signal and Information Processing" department since 2008. Since 2014 Thomas Zemen has been Senior Scientist at AIT Austrian Institute of Technology leading the research group for ultra-reliable wireless machine-to-machine communications. He is the author or coauthor of four books chapters, 30 journal papers and more than 80 conference communications. His research interests focus on reliable, low-latency wireless communications for highly autonomous vehicles; sensor and actuator networks; vehicular channel measurements and modeling; time-variant channel estimation; cooperative communication systems and interference management.
Dr. Zemen is an External Lecturer with the Vienna University of Technology and serves as Editor for the IEEE Transactions on Wireless Communications.